# On Monitoring Tearing Modes Stability in Toroidally Rotating Tokamak Equilibria

Enzo Lazzaro, Luca Bonalumi, Silvana Nowak, and Daniele Brunetti

***Abstract*— In tokamak operation, the control of dangerous MHD instabilities, possibly in real-time scenarios, must rely on prompt robust diagnostics of the state and stability of the system. The set of magnetic signals measured on the outside of the plasma boundary, based on the Zakharov–Shafranov, Shkarowsky, Wootton (ZSSW) current moments, has been always used for reliable monitoring of key characteristics of the instantaneous equilibrium condition, such as the quantities $\Delta_{Sh}$, the Shafranov centroid shift, $\beta_p$ related to the thermal energy content, and $l_i$ related to the current profile peakedness. In addition, the fast pickup coils monitor the external magnetic field fluctuations due to internal MHD activity, however, without the possibility of radial localization of the source. Here, we explore the potential usefulness of more complete use of ZSSW moments in association with the information from fast B perturbation signals to detect tearing stability conditions. For clarity, we set up an analysis of the measurable response to tearing perturbations based on an exact equilibrium model, which is an extension of the Solov'ev case with the addition of an equilibrium, nonuniform plasma rotation $\Omega(\psi)$. The relation of the selected (externally measurable) ZSSW moments to the calculated stability index is mapped for different rotation values. The footprint of the stability condition $\Delta' < 0$ on some current moments on the outer surface can then identify stability boundaries for different rotation conditions. This first discussion on an idealized exact model is proposed for testing the concept for application to realistic equilibria since it relies on a few externally monitorable quantities and very basic assumptions on the tearing modes physics.**

***Index Terms*— Bayes observer, current moments, tearing modes, tokamak.**

## I. Introduction

THIS work offers a contribution to the question of robust identification of some tokamak magnetic instabilities, which is crucial for the successful operation of the fusion oriented devices. Although the argument is based on well-known and well-developed physics, it is helpful for the reader to start with a nonpedantic concise summary of the relevant equilibrium conditions and a basic description of the tearing instability considered. In Section II, the notation is established, and a general tokamak equilibrium equation is derived a-new, including a steady rotation. Section III contains the explicit solution of Solov'ev type and its transformation to a parametric representation that allows easy construction of the metrics and identification of physical and geometric properties. In Section IV, the specific reconnection process at rational surfaces is succinctly described, focusing on the specific toroidal metrics effects on the current perturbation giving rise to the instability. The crucial argument on the scaling of the source of the instability is introduced and discussed. On this basis, in Section V, the concept of external magnetic measurements is revisited and extended; the solution of the homogeneous Grad–Shafranov equation in spherical coordinates is recalled to generate Zakharov–Shafranov, Shkarowsky, Wootton (ZSSW) [5] current moments; and the relation of generalized (externally measurable) ZSSW moments to the calculated stability index $\Delta'$ is mapped for different rotation values. The footprint of the stability condition $\Delta' < 0$ on some current moments on the outer surface [5], [14] can then identify stability boundaries, for different rotation conditions. The simplicity of the physical assumptions is believed to constitute a ground model that can be improved but not contradicted by more complete descriptions of the inner profiles. In Section VI, a Bayesian inference approach is used to test the theoretical detectability of the relevant information amidst the other measurements. In the conclusions, this first example based on an idealized analytical model is proposed for testing the method in view of application to realistic equilibria since it relies on few externally monitorable quantities and very basic assumptions on the T. M. physics.

Manuscript received May 29, 2020; revised November 13, 2020; accepted December 5, 2020. Date of publication December 30, 2020; date of current version January 11, 2021. This work was supported by the Euratom Research and Training Program 2014–2018 and 2019–2020 under Grant 633053. The review of this article was arranged by Senior Editor G. H. Neilson. *(Corresponding author: Enzo Lazzaro.)*

Enzo Lazzaro and Silvana Nowak are with the Institute for Science and Technology of Plasma (ISTP), Consiglio Nazionale delle Ricerche, 20125 Milan, Italy (e-mail: enzo.lazzaro@ist.cnr.it).

Luca Bonalumi is with the Dipartimento di Fisica "G.Occhialini," University of Milan-Bicocca, 20126 Milan, Italy.

Daniele Brunetti is with the Culham Centre for Fusion Energy, Culham Science Centre, Abingdon OX14 3DB, U.K.

Color versions of one or more figures in this article are available at https://doi.org/10.1109/TPS.2020.3043978.

Digital Object Identifier 10.1109/TPS.2020.3043978

## II. Basic Equilibrium Framework

The purpose of this work is to explore and eventually propose an extended use of the magnetic measurements taken outside the last closed magnetic surface (LCMS) of a tokamak to contribute to the means of continuous monitoring of the stability conditions of the configuration relative, in a first instance, to tearing perturbations. In order to set up the problem as clearly as possible, we find it convenient to choose as a demonstrative playground the geometry of the simplest, albeit not fully realistic, tokamak equilibrium, namely,

a variant of the Solov'ev type [1], [2]. In particular, we first rederive a solution of the Grad–Shafranov equation, including in the equilibrium a nonuniform toroidal rotation, and cast the solution in the inverse coordinate parametric representation that highlights simply the geometric characteristics of the configuration. The first step is to consider the steady-state, incompressible single-fluid MHD equations

$$\rho(\mathbf{v}\cdot\nabla\mathbf{v}) = \mathbf{J}\times\mathbf{B} - \nabla\mathbf{p} \tag{1}$$

$$-\nabla\Phi + \mathbf{v}\times\mathbf{B} = 0 \tag{2}$$

$$\nabla\cdot(\rho\mathbf{v}) = 0 \tag{3}$$

where the second equation represents Ohm's law, with $\Phi$ being the electrostatic potential. Due to axisymmetry and the incompressibility condition, the $\mathbf{B}$ field and the mass density flow can be written in the Clebsch notation as

$$\mathbf{B} = T\nabla\phi + \nabla\phi\times\nabla\psi \tag{4}$$

$$\rho\mathbf{v} = \Theta\nabla\phi + \nabla\phi\times\nabla F \tag{5}$$

where $T, F, \Theta, \Phi$ are all functions of the poloidal flux $\psi(R, Z)$ and, therefore, are constant on magnetic surfaces. Using expressions (4) and (5) in (2), with straightforward algebra, one obtains

$$\Phi' = \frac{1}{\rho R^2}[TF' - \Theta]. \tag{6}$$

The projection of the momentum balance equation (2) along the $\nabla\phi$-direction yields another surface quantity, from which a final expression for the flow velocity follows:

$$X(\psi) = T\left(1 - \frac{(F')^2}{\rho}\right) + R^2F'\Phi' \tag{7}$$

$$\mathbf{v} = \frac{F'}{\rho}\mathbf{B} - R^2\Phi'\nabla\phi. \tag{8}$$

The projection of the momentum balance equation (1) along $\mathbf{B}$ vanishes, and (6) and (8) yield the following relations:

$$\mathbf{B}\cdot\left[\frac{1}{2}(\nabla v^2) + \frac{\Phi'}{\rho}(F'T - \Phi'\rho R^2) + \frac{\nabla p}{\rho}\right] = 0. \tag{9}$$

Finally, (9) can be rewritten, using (6), as a generalized Bernoulli equation

$$\mathbf{B}\cdot\nabla\left[p + \rho\left(\frac{v^2}{2} + \Phi'\frac{\Theta}{\rho}\right)\right] = 0. \tag{10}$$

The quantity $P_s(\psi) = p + \rho((v^2/2) + \Phi'(\Theta/\rho))$ is a surface function; it is convenient to introduce the poloidal Mach number $M^2 \equiv (v_p^2/v_A^2) = ((F')^2/\rho)$ and write the projection of the momentum balance equation in the $\nabla\psi$ direction, obtaining the Grad–Shafranov equation generalized with the presence of a stationary toroidal plasma velocity $v_\phi = \Theta/R\rho$

$$(1-M^2)\,\triangle^*\psi - \frac{(M^2)'}{2}|\nabla\psi|^2 + \frac{1}{2}\left(\frac{X^2}{1-M^2}\right)' + R^2\left(P_s - \frac{XF'\Phi'}{1-M^2}\right)' + \frac{R^4}{2}\left(\frac{\rho(\Phi')^2}{1-M^2}\right)' = 0. \tag{11}$$

The Beltrami operator is explicitly $\triangle^*\psi = (\partial^2\psi/\partial R^2) - (2/R)(d\psi/dR) + (\partial^2\psi/\partial Z^2)$. In the absence of equilibrium flow, the Grad–Shafranov equation and the toroidal current density are

$$\triangle^*\psi = -\mu_0 R J_\phi \quad J_\phi = R\frac{dp}{d\psi} + \frac{T}{2\pi\mu_0 R}\frac{dT}{d\psi}. \tag{12}$$

In the following, we shall consider just the subsonic cases $M^2 \ll 1$ for which (11) remains elliptic. Comparison of (11) and (12) in the subsonic range leads to identify the current density in the presence of rotation

$$J_\phi = -\frac{1}{2\mu_0 R}(X^2)' + R(P_s - XF'\Phi')' + \frac{R^3}{2}(\rho(\Phi')^2)'. \tag{13}$$

### A. Paradigmatic Case With Exact Solution

In this section, (13) and (11) will be simplified choosing particular profiles. Although they might not picture a realistic situation, they provide a clear insight into the role and effects of the configuration geometry. In the following, we shall be concerned with external measurements that are generally considered rather "blind" to the internal features, but we can show that even the coarse description used can provide general conclusions. Noting that $X \to T$ and choosing

$$F' = 0 \tag{14}$$

$$T = \text{const} \tag{15}$$

$$\omega(\psi) = \frac{\Theta(\psi)}{\rho R^2} = -\Phi'(\psi) \tag{16}$$

$$p = p_0\left(1 - \frac{\psi}{\psi_b}\right) \tag{17}$$

$$\rho\omega^2 = \Omega_0\left(1 - \frac{\psi}{\psi_b}\right) \tag{18}$$

$$\Omega = \mu_0\Omega_0/2\psi_b \tag{19}$$

$$P_0 = \mu_0 p_0/\psi_b \tag{20}$$

where $[P_0] = [\mu_0\ Jl^{-1}]$ and $[\Omega = \mu_0\Omega_0/2\psi_b] = [\mu_0 l^{-5} q t^{-1} \approx \mu_0\ Jl^{-3}]$ labels the rotation effect on the current density; (12) becomes

$$\triangle^*\psi = -R^2P_0 - R^4\Omega. \tag{21}$$

Following the classical procedure by Solov'ev [1], an exact solution is obtained in the form:

$$\psi(R, Z) = c_0R^2Z^2 + k\left(R^2 - R_0^2\right)^2 + \alpha R^\beta. \tag{22}$$

After further dedimensionalization of (21), the coefficients and the final form of the solution are obtained, assigning boundary conditions $\psi = \psi_b = 4kR_0^2r_b^2$, going through the points $r = r_b$, $Z = Z_s = Z(r_b, \pi/2)$ and vanishing on the magnetic axis. With $k = ((Z_s(\mu_0\ p_0)^{1/2})/(4R_0\ r_b(2(Z_s^2 + r_b^2))^{1/2}))$ and $c_0 = (8r_b^2/Z_s^2)k$, one gets

$$\psi(R, Z) = c_0R^2Z^2 + k\left(R^2 - R_0^2\right)^2 + \frac{\Omega}{24}R^6 - \psi_{ax}. \tag{23}$$

The last constant makes the flux vanish at the magnetic axis and is $\psi_{ax} = (\Omega/24)R_0^6 - (\Omega^2/256k)R_0^8$. The poloidal $B_\theta$ field in rectified flux coordinates $(r, \theta, \phi)$ is $B_\theta(r) = (\psi'(r)/\sqrt{g})$, where $\sqrt{g}$ is the Jacobian of the transformation from the $(R\cdot\phi, Z)$ coordinates. Simple but crucial observation should be made on the structure of the current density on

the right-hand side of (21). It is basically an expression of the fundamental force balance in toroidal geometry and is strictly related to the geometric and global properties of the equilibrium configuration, which are efficiently identified by "moments" measured outside the plasma; toroidicity and shaping help removing certain degeneracies, allowing, for instance, separation of $\beta_p$ and $\ell_i$ [4], [15]. The first conjecture is that this "irreducible" toroidal effect may carry also other global information, so far disregarded, related to certain stability conditions.

### *B. Parametric Representation of Exact Solution and Metric Coefficients*

The exact solution (23) can be usefully represented in the general parametric form [3]

$$R(r,\theta) = R_{ax} + (R_1(r) + R_{11}(r,\Omega))\cos\theta + R_2(r)\cos 2\theta - \delta \tag{24}$$

$$Z(r,\theta) = (Z_1(r) + Z_{11}(r,\Omega)\sin\theta \tag{25}$$

where $r$ is a flux surface function, and $\theta$ is a rectified poloidal angle variable. From (24) and (25), the metric tensor $g_{ik}$ is easily calculated analytically, to be used in writing the equation for the helical magnetic perturbations, in full toroidal geometry. For simplicity, we show, in the Appendix, the explicit expressions of the coefficients of (24) and (25) and display the relevant metrics later on when needed. A fair amount of tedious algebra is unavoidable to be able to evaluate consistently some moments of the interior current profile and some contour integrals on the plasma outer boundary, thereby proving our statements, anticipated in the introduction.

## III. External Magnetic Measurements

The tokamak toroidal current density distribution, $J_\phi(\mathbf{r})$, is a continuous function of points $\mathbf{r}$ of coordinates $(R, Z)$, compact within the domain (set of points) S bounded by the LCMS. For convenience, in the following, we shall use the normalized profile $\widehat{J_\phi}(\mathbf{r}) \simeq \mathbf{J}_\phi(\mathbf{r})\mathbf{S}_\phi/\mathbf{I}$, where $I$ is the total current and $S_\phi$ a toroidal cross section. Consider a complete numerable set $\Re$ of real-valued orthonormal basis functions $u_n(\mathbf{r})$; the normalized function $\widehat{J_\phi}(\mathbf{r})$ could be represented by an expansion in $u_n(\mathbf{r})$, in the form of a smooth (integral) superposition of filaments

$$\widehat{J_\phi}(\mathbf{r}) = \int \mathbf{dr}' \sum_n^\infty C_n u_n(r'))\delta(\mathbf{r}-\mathbf{r}') \tag{26}$$

and the reconstruction of the current profile, albeit approximate, in principle, could be expected to consist in determining the weighting coefficients $C_n$ by finding a large enough number $N$ of external measurements to be matched to $N$ boundary values of $u_n(\mathbf{r_b})$, obviously under the constraint that $\sum_n^N C_n u_n(\mathbf{r_b}) = \mathbf{0}$, with the integral value constrained by the measured total current $I$. However, this procedure cannot be even formally pursued, outside the general formulation of a suitably regularized inverse MHD equilibrium problem [13]. The use of external magnetic diagnostics has nonetheless proved to be a powerful and robust tool to determine several important characteristics of the tokamak configuration, such as the plasma position and shape, associated with the $J_\phi$ profile and the boundary conditions. Shafranov [4] and Zakharov and Shafranov [5] first showed that multipole moments of current density are given by closed-contour integrals of the external magnetic field and how these moments are related to plasma position and shape. Their analysis limited to the case of symmetry with respect to the midplane and first order in $\epsilon = r/R$ was later expanded by other authors [6]–[9], always with the objective of a robust identification of the geometrical characteristics of the plasma meridian cross section. In the work in [5] and [7]–[9], the solution of the homogeneous Grad–Shafranov equation, valid in vacuum, is expressed in terms functions of the type $f^{(m)}(\rho,\mu) = \rho^{m+1}(1-\mu^2)^{1/2}P_m^1(\mu)$ (where $\rho^2 = R^2 + Z^2$, $\mu = \cos\theta$), related to associated Legendre polynomials, and it is shown that the $m$th moments of the internal current profile $J_\phi$, defined in [5], [8], and [9], are equal to weighted contour integrals of the peripheral magnetic field tangent and normal components on closed paths, surrounding the plasma

$$Y_m = \frac{1}{\mu_0 I}\int J_\phi f_m dS_\phi = \frac{1}{\mu_0 I}\oint f_m B_\theta(r_b) d\ell = \frac{1}{\mu_0 I}\int_0^{2\pi} f_m B_\theta(r_b)\sqrt{g_{\theta\theta}(r_b)}\, d\theta. \tag{27}$$

For convenience, the set of functions $f^{(m)}(R, Z)$ is changed into an equivalent set $f_m(\mathrm{x}, \mathrm{Z})$ vanishing on the magnetic axis, and for the sake of argument, the integration contour is the plasma boundary, at $r = r_b$. In the following, the moments 27 of interest shall be those generated by the functions of [9]:

$$f_1 = x\left(1 + \frac{x}{2R_0}\right) \tag{28}$$

$$f_2 = Z\left(1 + \frac{x}{R_0}\right)^2 \tag{29}$$

$$f_3 = x^2\left(1 + \frac{x}{2R_0}\right)^2 - Z^2\left(1 + \frac{x}{R_0}\right)^2 \tag{30}$$

$$f_4 = \left[2Zx\left(1 + \frac{x}{2R_0}\right) - \frac{4}{3}\frac{Z^3}{R_0}\right]\left(1 + \frac{x}{R_0}\right)^2 \tag{31}$$

$$f_5 = x^3\left(1 + \frac{x}{2R_0}\right)^3 - 3xZ^2\left(1 + \frac{x}{2R_0}\right)\left(1 + \frac{x}{R_0}\right)^2 + \frac{Z^4}{R_0}\left(1 + \frac{x}{R_0}\right)^2 \tag{32}$$

$$f_6 = \left[3Zx^2\left(1 + \frac{x}{2R_0}\right)^2 - Z^3\left(1 + \frac{6x}{R_0} + \frac{3x^2}{R_0^2}\right) + \frac{6}{5}\frac{Z^5}{R_0^2}\right] \times \left(1 + \frac{x}{R_0}\right)^2. \tag{33}$$

## IV. Linear Tearing Modes Perturbations

The first-order helical perturbations of the type $\widetilde{f}(r,\theta,\phi) = \widetilde{f}(r)_{m,n}e^{i(m\theta - n\phi)}$ in current density may lead to magnetic instabilities growing around the closed field lines, rational $q$ surfaces and generating the externally measured, time periodic "Mirnov" signals. Eventually, the instability transforms nonlinearly in finite size magnetic islands, whose evolution,

up to the saturation stage, largely depends on the linear growth rate. The latter is governed by a dispersion relation of the type

$$\Delta' = \Delta'_{\text{layer}} \tag{34}$$

where $\Delta'_{\text{layer}}$ depends on the physics of magnetic reconnection within the inner layer around $r = r(q = m/n)$, and the "external" $\Delta' = ((d\ln(\widetilde{\psi}_{m,n}))/dr)|_{r(q=m/n)}$ results from the solution of the tearing equation. Considering linear perturbations of current and magnetic field

$$\mathbf{J} = \mathbf{J_0} + \widetilde{\mathbf{J}}_\mathbf{1} \tag{35}$$

$$\mathbf{B} = \mathbf{B_0} + \widetilde{\mathbf{B}}_\mathbf{1}. \tag{36}$$

The condition of vanishing torque density $\nabla \times (\mathbf{J} \times \mathbf{B}) = \mathbf{0}$ is expressed in the equation for the first-order perturbed helical poloidal flux $\widetilde{\psi}_{m,n}$, which, in curvilinear (toroidal) geometry, takes the form

$$\left\langle \frac{g_{\theta\theta}}{\sqrt{g}} \right\rangle \frac{\partial^2 \widetilde{\psi}_{m,n}}{\partial r^2} + \left\langle \frac{g_{\theta\theta}}{\sqrt{g}} \right\rangle' \frac{\partial \widetilde{\psi}_{m,n}}{\partial r} - \left[ m^2 \left\langle \frac{g_{rr}}{\sqrt{g}} \right\rangle + \frac{m}{m - nq} \langle J^* \rangle' \right] \widetilde{\psi}_{m,n} = 0. \tag{37}$$

In the explicit form, in this basic configuration, we have the following dependence on the geometry, pressure, and rotation:

$$\left\langle \frac{g_{\theta\theta}}{\sqrt{g}} \right\rangle = \frac{4\sqrt{2} r (c_0 + 8k)}{33 R_0 \sqrt{c_0 k}} + \frac{\Omega R_0 r (c_0 + 8k)}{44 \sqrt{2 c_0 k^3}} \tag{38}$$

$$\left\langle \frac{g_{\theta\theta}}{\sqrt{g}} \right\rangle' \Big/ \left\langle \frac{g_{\theta\theta}}{\sqrt{g}} \right\rangle = \frac{1}{r} \tag{39}$$

$$\left\langle \frac{g_{rr}}{\sqrt{g}} \right\rangle \Big/ \left\langle \frac{g_{\theta\theta}}{\sqrt{g}} \right\rangle = \frac{1}{r^2}. \tag{40}$$

Ultimately, the source of tearing mode depends on the perturbation of the physical current density near the rational surface, which is related to the contravariant toroidal current by $J_{0\phi} = (g_{\phi\phi})^{1/2} J_0^\phi$, where $(g_{\phi\phi})^{1/2} = R$

$$J_{\phi,1} \equiv J^\star \propto \frac{J_{0\phi}}{T} R. \tag{41}$$

Near the rational surface $r = r_s$, the strength of driving term of the tearing perturbation in (37) in the present test case can be explicated as

$$J^\star = -AR^2 - BR^4 \tag{42}$$

where the equilibrium current used here is given by the expression consistent with (21) and $A = (P_0/T)$, $B = (\Omega/T)$. In Section IV-A, for the sake of argument, we focus on the scaling of the current perturbation with the characteristics of this equilibrium, which, albeit particular [see (21) and (23)], keeps track of the fundamental toroidal metrics underlying also any more detailed equilibrium current profile. As argued earlier, it is worth searching how the associated information may be linked to the stability condition.

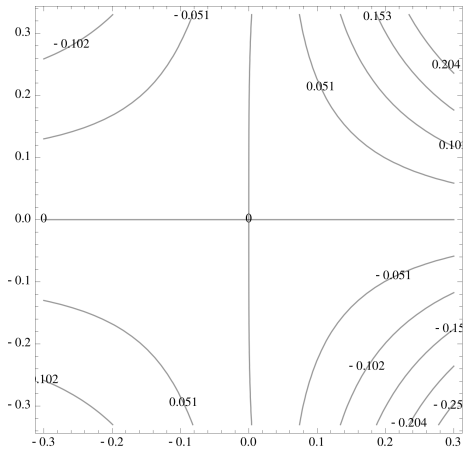


Fig. 1. Contour plot in the $(x, Z)$ plane, of $f_4$ multipolar function, associated with the elongation $\kappa$.

### A. Multipolar Moments of Tearing Current Density Perturbation

In this section, we shall investigate whether a generic tearing current perturbation "$J^\Delta$" leaves a specific, and detectable, multipolar "footprint" on an outer contour (e.g., LCMS) and construct applicable, albeit approximate expressions. We can conjecture a scaling of the perturbation $J^\Delta(r, \theta, \Omega) \propto AR^\lambda + BR^\nu$, where the exponents $\lambda$ and $\nu$ are determined by the expected equilibrium current profile. A moment associated with the "tearing source" $J^\Delta$ can be defined as

$$Y^\Delta = \frac{1}{\mu_0 I} \oint f^\Delta B_\theta(r_b) d\ell = \frac{\psi'(r_b)}{\mu_0 I} \oint f^\Delta \frac{\sqrt{g_{\theta\theta}(r_b)}}{\sqrt{g(r_b)}} d\theta. \tag{43}$$

From the general structure [9] of the $f^{(m)}$, solutions of $\triangle^\star f^{(m)} = 0$, it results that some linear combination of the functions $f^{(1)}$, $f^{(3)}$ $f^{(5)}$ scaling as $-(1/2R_0)R^2$, $(1/4R_0^2)R^4$, and $-(15/8)R^6$ can be useful to define a moment related to $\Delta'$

$$f^\Delta \approx \alpha f^{(1)} + \beta f^{(3)} \approx -AR^\lambda - BR^\nu. \tag{44}$$

In the specific case of (41), we have $\lambda = 2$ and $\nu = 4$. By matching the terms with corresponding powers of $R$ (44) $R^4$, the constants are determined as $\alpha = -2R_0(P_0/T)$ and $\beta = -4R_0^2(\Omega/T)$, leading eventually to the practical definitions

$$f_\Delta := -2R_0 \frac{P_0}{T} f_1 - 4R_0^2 \frac{\Omega}{T} f_3 \tag{45}$$

and from 43

$$Y^\Delta = -\frac{2R_0 \psi'(r_b)}{\mu_0 I} \oint \left[ \frac{P_0}{T} f_1 + 2R_0 \frac{\Omega}{T} f_3 \right] \frac{\sqrt{g_{\theta\theta}(r_b)}}{\sqrt{g(r_b)}} d\theta. \tag{46}$$

Figs. 1 and 2 show the contour plots of the weight functions $f_4$, associated with elongation, and $f_\Delta$. It is expected that information of the internal "tearing source" is conserved in the mapping provided by the surface moments. Correspondence between the relevant measured moment and $\Delta'$ can be established by numerical calculations, up to an irrelevant multiplication factor. Stability domains can be constructed in operating spaces $(c_0, T)$ and $(k, T)$ for different

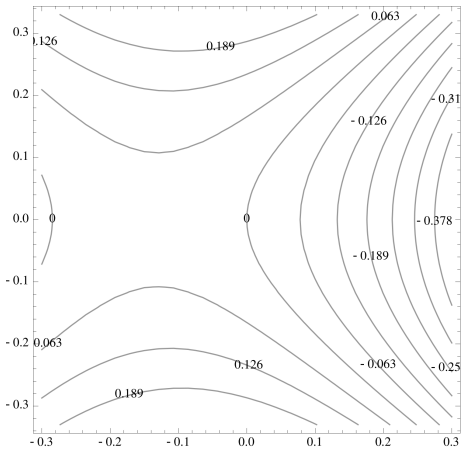


Fig. 2. Contour plot in the $(x, Z)$ plane, of $f_\Delta$ multipolar function.

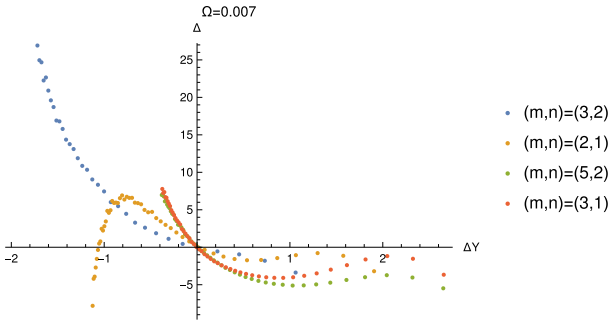


Fig. 3. Plot of $\Delta'$ versus $\Delta Y_\Delta$ for a range of modes $(m, n)$ at a fixed value of the toroidal rotation label $\Omega = 0.007$ [see definition 19]; $\Delta Y_\Delta \geq 0$ is associated with $\Delta' \leq 0$.

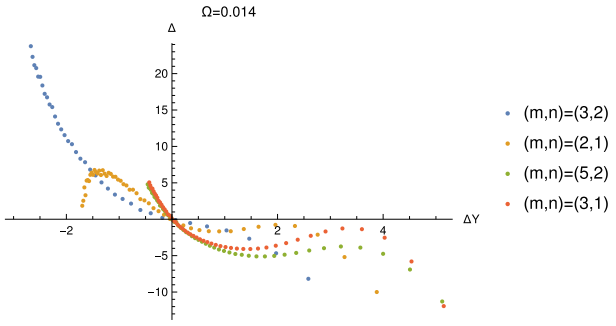


Fig. 4. Plot of $\Delta'$ versus $\Delta Y_\Delta$ for a range of modes $(m, n)$ at a fixed value of the toroidal rotation label $\Omega = 0.014$ [see definition 19].

$(m, n)$ modes and toroidal rotation $\Omega$. In order to test sensitivity, the strict choice of the source $J^*$ model of (42) could be relaxed, with different values of $\lambda$ and $\nu$, leading to different linear combinations of $f_m$, which can show higher sensitivity to $\Delta'$. An example is discussed in Section V for $\lambda = 4, \nu = 6$, and $\widehat{f_\Delta} := 4\ R_0^2 A f_3 + 8\ R_0^3 B f_5$.

## V. Sensitivity and Stability Domains

The stability parameter $\Delta'$ is calculated solving numerically the tearing equation (37). The results of the physical model are shown in Figs. 3–8.

The correlation of the tearing linear instability parameter $\Delta'$, with the externally measurable moment $Y_\Delta$, here is more

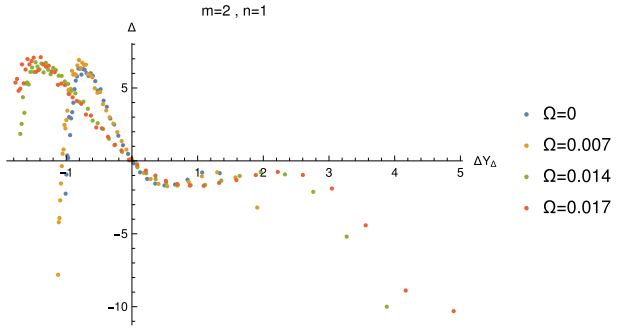


Fig. 5. Plot of $\Delta'$ versus $\Delta Y_\Delta$ f for mode $m = 2$, $n = 1$ at different values of the toroidal rotation label $\Omega$ in the range $0 \leq \Omega \leq 0.017$; $\Delta Y_\Delta \geq 0$ is associated with $\Delta' \leq 0$.

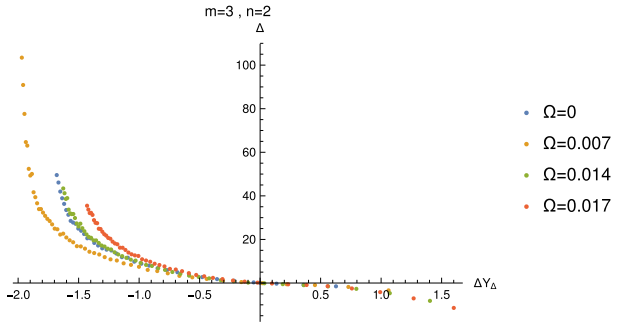


Fig. 6. Plot of $\Delta'$ versus $\Delta Y_\Delta$ for mode $m = 3, n = 2$ in the toroidal rotation range $0 \leq \Omega \leq 0.017$.

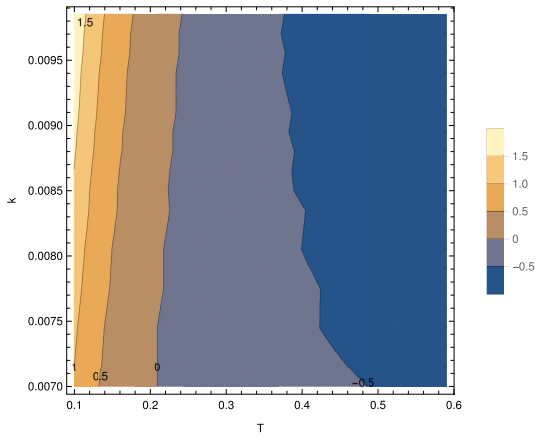


Fig. 7. Domain of stability identified by $\Delta Y_\Delta$ versus $T, k$. The region $\Delta Y_\Delta \geq 0$ is stable.

conveniently displayed by plotting it versus $\Delta Y_\Delta = Y_\Delta - Y_{\Delta=0}$, for a range of mode numbers $(m, n)$, as shown in Figs. 3 and 4, for two fixed values of rotation $\Omega$. The relation of $\Delta'$ with $\Delta Y_\Delta = Y_\Delta - Y_{\Delta=0}$, for modes $m = 2, n = 1$ and $m = 3, n = 2$, is shown in Figs. 5 and 6 for different values of the toroidal rotation $\Omega$. It is apparent that the change of sign of $\Delta Y_\Delta$ is the same as that of $\Delta'$, irrespective of the rotation: this makes this signal very suitable to monitor the (linear) stability condition.

The analysis in Figs. 3–6 is done for $k = 0.007$, $c_0 = 0.05$, $R_0 = 1.9$, $r_b = 1$, $\Omega = 0.007$, and $p_0 = 0.1$. It is possible to build the stability domains in the parameters space $(c_0, k, T)$, and the data are summarized in two contour plots.

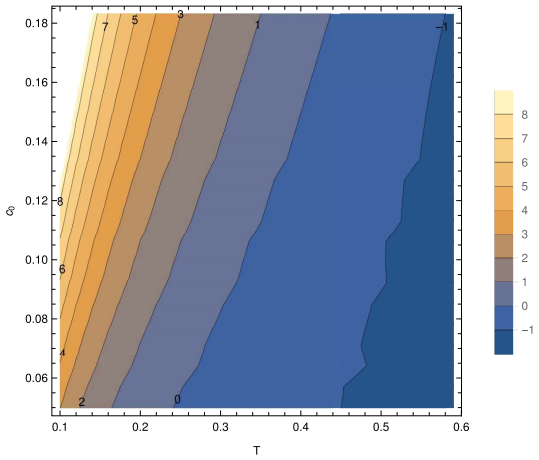


Fig. 8. Domain of stability identified by $\Delta Y_\Delta$ versus $T, c_0$. The region $\Delta Y_\Delta \geq 0$ is stable.

In Fig. 7, the parameter range is $0.007 < k < 0.01$; in Fig. 8, $0.05 < c_0 < 0.19$; and in both cases, $0.1 < T < 0.6$. Figs. 7 and 8 show that, in the upper limit of the range of $k$ and $c_0$, the moment $\Delta Y_\Delta$ becomes larger, corresponding to a more stable equilibrium. This is consistent with the behavior of $\Delta'$ calculated using the exact equilibrium.

As a test of sensitivity to uncertainty in the basic structure of the $J*$ source, here, we summarize the case with $\lambda = 4$ and $\nu = 6$ related to a different profile, not consistent with the equilibrium (23). Expression (46) is evaluated choosing, arbitrarily, the parameters $m = 3, n = 2, k = 0.007, c_0 = 0.05, R_0 = 1.9, r_b = 1, \Omega = 0.007$, and $p_0 = 0.1$. The parameter $T$ modifies only the profile of the safety factor $q$; in this way, the geometry of the system is kept fixed. For each couple of values $(c_0, k)$, the value of the $Y_\Delta = 0$ is calculated and subtracted from $Y_\Delta$. Note that, in this case, the sign of $\Delta Y_\Delta$ is the same as that of $\Delta'$. In the table, the sensitivity result is reported.

| $T$ | $\Delta'$ | $Y_\Delta$ | $\Delta Y_\Delta$ |
|---|---|---|---|
| 0.14 | -0.0758541 | -36.8296 | 0. |
| 0.1 | -3.37647 | -52.5915 | -15.7619 |
| 0.11 | -1.80164 | -47.8105 | -10.9809 |
| 0.12 | -0.947699 | -43.8263 | -6.99665 |
| 0.13 | -0.55219 | -40.455 | -3.6254 |
| 0.14 | -0.0758541 | -37.5654 | -0.735759 |
| 0.15 | 0.443696 | -35.061 | 1.7686 |
| 0.16 | 1.12254 | -32.8697 | 3.95991 |
| 0.17 | 1.87055 | -30.9362 | 5.89342 |
| 0.18 | 2.61012 | -29.2175 | 7.6121 |
| 0.19 | 3.28078 | -27.6797 | 9.14986 |

It can, therefore, be confirmed that external magnetic measurements with rather flexible combinations of $f_m$ multipolar weight functions can monitor the $\Delta'$ stability condition.

## VI. Source and Signals

In the previous sections, the basic scaling of the metrics' effect on the "tearing mode" current perturbation was inferred, and it has been shown how a certain linear combination (possibly not unique) of the externally measurable $Y_m$ is sensitive to the TM stability index $\Delta'$. An important question remains open, namely that concerning the detectability of this information amidst that provided by the other moments and the background noise. To address this question, at least in a preliminary way, we have to introduce elements of information theory and statistical decision techniques. For the specific purpose of modeling the "origin" of TM perturbations, to be "coded" onto externally measurable magnetic signals, because of the unknown nonmetrical effects, it is proposed to consider the current distribution as "source" of the multipolar moments $Y_m$ defined in (27), along the lines of [9] as a set of independent random variables. One can consider a discrete subset of $n$ generalized multipoles $Z_i = \int \widehat{J}_\phi L(f_i) dS_\phi$, where $L(f_i)$ is a linear combination more directly associated with physical quantities [8], [9]. The symbol $Z_1$ is associated with the Shafranov shift $\Delta_{\text{Shaf}}$, while combinations $Z_\kappa \approx L(Y_3, Y_4)$ are associated with the elongation $\kappa$, and $Z_\delta \approx L(Y_5, Y_6)$ are related with the triangularity $\delta$ of the plasma configuration [9]; in the present case, we are interested in $Z_\Delta = \alpha Y_1 + \beta Y_3$. On the basis of a statistical framework, we can address the problem of assessing the detectability of the signal of interest.

### A. Statistical and Probabilistic Model

More specifically, we can picture the current as a "source" of $n$ moments [see (27)] with amplitudes that are random variables described by "prior" probability distributions, taken, without loss of generality, to be normal density distributions $\Phi_N(Z_m|\mu_m, \sigma_m)$, with mean $\mu_m = Z_m$ and unspecified standard deviation $\sigma_m$. Then, by reordering and subdividing the sequence $Z_{\min}, \ldots, Z_m \ldots, Z_{\max}$, we evaluate the probabilities of the "symbols" $Z_m$ as

$$P_1(-\infty \leq Z \leq Z_1) = \int_{-\infty}^{Z_1} \Phi_N(y) dy \tag{47}$$

$$P_k(Z_k \leq Z \leq Z_{k+1}) = \int_{Z_k}^{Z_{k+1}} \Phi_N(y) dy \tag{48}$$

$$P_m(Z_m \leq Z \leq \infty) = \int_{Z_m}^{\infty} \Phi_N(y) dy. \tag{49}$$

In order to assess the relevance of the information of the symbol $Z_\Delta$ in comparison with the other moments, here, we follow a rather elementary line of reasoning. We estimate the conditional probability that the message generated by the source is "$Z_\Delta$ when $Z_\kappa$" is also observed. The Bayes theorem gives the conditional probability

$$P(Z_\Delta \mid Z_\kappa) = P(Z_\kappa \mid Z_\Delta) \times P(Z_\Delta)/P(Z_\kappa) \tag{50}$$

where $P(Z_\kappa \mid Z_\Delta)$ is the likelihood function of detection of $Z_\Delta$ when symbol $Z_\kappa$ has been detected, and $P(Z_\kappa \mid Z_\Delta) \times P(Z_\Delta)$ is the "posterior" probability of symbol $Z_\Delta$, while $P(Z_\kappa)$ is the "evidence," which amounts to a normalization constant. Eventually, by ordering the posterior probabilities, the relevance of the information of the $Z_\Delta$ symbol can be assessed. In the language of information theory, the ensemble of $Z_i$ is the set of N "symbols," ("letters") of the "alphabet" A, of the "source" [17], which generates random variables each with a probability $P_i$. A string of "letters," "symbols" is

an elementary event, "message" in probability space, and is a random process.

### *B. Likelihood Ratio and Ideal Observer Analysis*

We want to formulate the problem of detectability of a specific moment (symbol), say $Z_\Delta$ in the presence of at least another signal (message), say $(Z_1, Z_\kappa, Z_\delta)$; in general, one should consider detectability against background noise, but, here, for the sake of argument, it is sufficient just the comparing between the noiseless signals. The task is to discriminate between two classes of moments that can be measured; we label as "class 0" the set of symbols $\mathbf{Z}_j$, $(j = 0, 1)$ that do not include the information about $\Delta'$, and "class 1" that does include it. The optimal discriminator of two classes of symbols, with probability densities $p_j(\mathbf{Z}_j)$, is given by the Bayesian ideal observer [22], [23], expressed in terms of the likelihood ratio (or the log-likelihood ratio) [see (50)]. In the present case, $Z_{j,i}$ $(i = 1, n)$ are samples of size $n = 4$ from normal density distributions $p_j(\mathbf{Z}_j) = \Phi_N(\mathbf{Z}_j|\mu, \sigma)$, with mean and variance, $\mu$ and $\sigma$, determined by seeking maximum likelihood, for given "data" $\mathbf{Z}_j$, for each class $j$. The mean value and the value $\widehat{\sigma}^2$ that maximize the likelihood function

$$L_n(\mathbf{Z}_j \mid \mu, \sigma) = \left(\frac{1}{\sqrt{2\pi}\,\sigma}\right)^n \exp\left[-\frac{1}{2}\frac{\sum_{i=1}^n (Z_i - \mu)^2}{\sigma}\right] \quad (51)$$

turn out to be

$$\widehat{\mu} = \overline{Z} = \frac{1}{n}\sum_i^n Z, \quad \widehat{\sigma}^2 = \frac{1}{n}\sum_i^n (Z_i - \widehat{\mu})^2 \quad (52)$$

$$L_n(\widehat{\mu}, \widehat{\sigma}) = \left(\frac{1}{\sqrt{2\pi}\widehat{\sigma}}\right)^n e^{-\frac{n}{2}}. \quad (53)$$

For class 0, $\widehat{\mu} = \mu_0$, and for class 1, $\widehat{\mu} = \mu_1$. The likelihood ratio statistic is defined as

$$\Lambda(\mu, \sigma) = \frac{L_{n,0}(\mathbf{Z_0}|\mu_0, \sigma_0)}{L_{n,1}(\mathbf{Z_1}|\mu_1, \sigma_1)} = \left(\frac{\sigma_1^2}{\sigma_0^2}\right)^{\frac{n}{2}} = \left(\frac{\sum_i^n (Z_i - \overline{Z})^2}{\sum_i^n (Z_i - \mu_0)^2}\right)^{\frac{n}{2}}. \quad (54)$$

As a particular test case, we consider the discrimination of a "message" string of length $n = 6$, including the $Y_4$ moment, associated with elongation, and no $Z_\Delta$, and one with $Z_\Delta$ in place of $Y_4$. The sample means are $\mu_0 = (1/n)(Y_1 + Y_2 + Y_3 + Y_4 + Y_5 + Y_6)$ and $\mu_1 = (1/n)(Y_1 + Y_2 + Y_3 + Z_\Delta + Y_5 + Y_6)$. We can apply the analysis formulating the null hypothesis $\mathbf{H_0}$ in relation to the detection of the value of one parameter, typically the mean, $\mu_0$, of the $p_0$ distribution and the alternative $\mathbf{H_1}$ associated with $\widehat{\mu} = \mu_1 \neq \mu_0$. Intuitively, if the evidence (data) supports $\mathbf{H_1}$, then the likelihood function $L_{n,1}(\mathbf{Z_1}|\mu_1)$ should be large; therefore, the likelihood ratio $\Lambda$ is small. Thus, the null hypothesis $\mathbf{H_0}$ is rejected, and the symbol $Z_\Delta$ is detectable. The rejection region for $\mathbf{H_0}$ (acceptance for $\mathbf{H_1}$) is $\Lambda \leq \widehat{k}$, which is some threshold and, after some manipulation of (54), translated into a t-Student test criterion for the statistics $t = \sqrt{n}(\overline{Z} - \mu_0/S > \widehat{k'}$, with the standard deviation estimator $S^2 = (1/(n-1))\sum_i^n (Z_i - \mu_0)^2$. The level of significance of the null hypothesis at 5% occurs if $t > 1.96$.

| $\mu_0$ | $\mu_1$ | $\sigma_0$ | $\sigma_1$ | $S$ | $t$ |
|---|---|---|---|---|---|
| $-0.495$ | $-0.081$ | 1.40 | 0.963 | 0.43 | 2.35 |

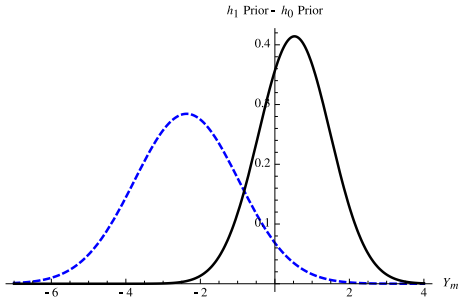


Fig. 9. Prior probability distributions of $Y_4$ and $Z_\Delta$ for $H_0$ and $H_1$.

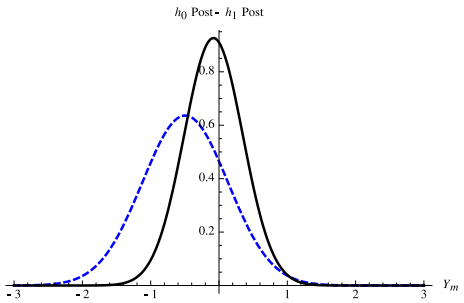


Fig. 10. Plot of posterior probability distributions of $Y_4$ and $Z_\Delta$ for $H_0$ and $H_1$.

Furthermore, another discriminating parameter is the distance of the peaks of the posterior density functions, divided by the standard error estimate $d' \equiv ((\mu_1 - \mu_0)/S) \approx 0.422$. Hence, the moment $Z_\Delta$ should be reasonably observable in an experimental situation, even in the presence of the measurements of the other moments, typically the moments associated with the elongation. A plot of prior and posterior probability distributions [see 50] for $Y_4$ and $Y_\Delta$ is shown in Figs. 9 and 10. By construction, it is clear that rotation enhances a discriminating effect even though the change of sign of $Y_\Delta$ with $\Delta'$ appears largely independent of rotation, for all modes, as shown in Figs. 5 and 6.

Other combinations of moments, such as $\widehat{f}_\Delta$, presented previously, monitor as well the sign of $\Delta'$ and are more detectable. This indicates sufficient freedom for applications.

## VII. Conclusion

A new approach has been presented to the problem of detection of meaningful characteristics of a tokamak configuration, based on the simplest, but fully toroidal model of equilibrium, Solov'ev-like, but with rotation. The detectability of the sign of $\Delta'$ is clearly enhanced by the effect of rotation. Exploiting the vacuum solution of the field equation in terms of the Legendre functions, some new, relevant information on the tearing stability conditions has been shown to be associated with combinations of externally measurable multipole moments. The choice of combinations is not unique, but several can be sensitive to the sign of $\Delta'$. By a

statistical approach, a procedure of the Bayesian inference has been used to ascertain the "theoretical" detectability of the relevant multipole moment. Given the simplicity of the assumptions, the procedure can be applied to more refined theoretical models and, especially, can be tried on real experimental measurements, where no detailed knowledge of the internal current profile is available.

## APPENDIX

### Evaluation of Coefficients of the Parametric Representation

The solution (23) can be usefully represented in the general parametric form [3], in a mildly nonuniform current approximation

$$R(r,\theta) = R_{ax} + (\epsilon R_1 + \epsilon^2 R_{11})\cos\theta + \epsilon^2 R_2 \cos 2\theta - \delta\epsilon^2 \tag{55}$$

$$Z(r,\theta) = (\epsilon Z_1 + \epsilon^2 Z_{11})\sin\theta \tag{56}$$

with $\epsilon \sim (r/R_0)$ being an ordering tag, eventually set to 1. A system of equations can be built evaluating the moments of the solution $\psi(R(r,\theta), Z(r,\theta))$

$$\int_0^{2\pi} \epsilon^2 \bar{\psi}\cos n\theta d\theta = \int_0^{2\pi}\left[c_0 R^2 Z^2 + k\left(R^2 - R_0^2\right)^2 + \frac{\Omega\psi}{24}R^6 - \psi_{ax}\right]\cos n\theta d\theta \tag{57}$$

where the term $\bar{\psi}$ is now seen as a labeling variable that scales as $r^2 \sim \epsilon^2$ and denotes a specific magnetic surface. The same order terms are equated to obtain the coefficients of (55) and (56)

$$R_1 = r, \quad R_{11} = -\frac{\Omega R_0^2 r}{32k}, \quad R_2 = \frac{r^2}{4R_0} \tag{58}$$

$$Z_1 = \frac{2\sqrt{2k}r}{\sqrt{c_0}}, \quad Z_{11} = \frac{\Omega R_0^2 r}{8\sqrt{2c_0 k}}, \quad \delta = \frac{3r^2}{4R_0}. \tag{59}$$

Further steps are needed to ensure that the LCMS remains fixed. The boundary conditions have to be imposed to enforce independence from the parameter $\Omega$

$$R(r_b,0)|_{\Omega=0} = R(r_b,0), \quad R(r_b,\pi)|_{\Omega=0} = R(r_b,\pi) \tag{60}$$

$$Z\left(r_b,\frac{\pi}{2}\right)|_{\Omega=0} = Z\left(r_b,\frac{\pi}{2}\right), \quad \beta_p|_{\Omega=0} = \beta_p. \tag{61}$$

The coefficients $k$, $c_0$, $R_0$, and $r_b$ are functions of toroidal flow $\Omega$. The system is solved after a linearization of these coefficients

$$k = k_0 + \epsilon k_1, \quad R_0 = R_{00} + \epsilon R_{01} + \epsilon^2 R_{02} \tag{62}$$

$$c_0 = c_{00} + \epsilon c_{01}, \quad r_b = r_{b0} + \epsilon r_{b1}. \tag{63}$$

Thus, the system yields

$$R_{00} = R_0, \quad R_{01} = \frac{\Omega R_0^3}{32k}, \quad R_{02} = \frac{(7c_0 + 24k)\Omega^2 R_0^5}{2048k^2(c_0 + 8k)} \tag{64}$$

$$c_{00} = c_0, \quad c_{01} = \frac{c_0 \Omega R_0^2}{2c_0 + 16k} \tag{65}$$

$$k_0 = k, \quad k_1 = -\frac{(c_0 + 4k)\Omega R_0^2}{8(c_0 + 8k)} \tag{66}$$

$$r_{b0} = r_b, \quad r_{b1} = \frac{\Omega r_b R_0^2}{32k}. \tag{67}$$

Using (58), (59), and (64)–(67), the final form of the parametric representation (55) and (56) can be written as

$$R(r,\theta) = R_0 + \epsilon r\cos\theta - \epsilon^2\frac{r^2(8\sin^2\theta - \cos 2\theta + 3)}{4R_0} - \epsilon^2\frac{\Omega r R_0^2\cos\theta}{32k} \tag{68}$$

$$Z(r,\theta) = \epsilon\frac{2\sqrt{2}\sqrt{k}r\sin\theta}{\sqrt{c_0}} + \epsilon^2\frac{\sin\theta\left(64kr^2\cos\theta - \Omega r R_0^3\right)}{8\sqrt{2c_0 k}}. \tag{69}$$

From (68) and (69), one can calculate the metric tensor used in (37) and (46).

## ACKNOWLEDGMENT

This work has been carried out within the framework of the EUROfusion Consortium. The views and opinions expressed herein do not necessarily reflect those of the European Commission.

## REFERENCES

[1] L. S. Solov'ev, "The theory of hydromagnetic stability of toroidal plasma configurations," *J. Exp. Theor. Phys.*, vol. 26, no. 2, p. 400, 1968.

[2] H. Tasso and G. N. Throumoulopoulos, "Axisymmetric ideal magnetohydrodynamic equilibria with incompressible flows," *Phys. Plasmas*, vol. 5, pp. 2378–2383, Jun. 1998.

[3] L. Lao, S. P. Hirshman, and R. M. Wieland, "Variational moment solutions to the Grad–Shafranov equation," *Phys. Fluids*, vol. 24, pp. 1431–1440, Aug. 1981.

[4] V. D. Shafranov, "Determination of the parameters $\beta_I$ and $l_i$ in a Tokamak for arbitrary shape of plasma pinch cross-section," *Plasma Phys.*, vol. 13, pp. 757–762, 1971.

[5] L. E. Zakharov and V. D. Shafranov, "Integral relations for an equilibrium toroidal plasma filament with a noncircular cross section," *Zhurnal Tekhnicheskoi Fiziki*, vol. 43, p. 225, Feb. 1973.

[6] A. J. Wootton, "Measurements of plasma shape in a tokamak," *Nucl. Fusion*, vol. 19, p. 987, Jul. 1979.

[7] M. F. Reusch and G. H. Neilson, "Toroidally symmetric polynomial multipole solutions of the vector laplace equation," *J. Comput. Phys.*, vol. 64, no. 2, pp. 416–432, Jun. 1986.

[8] I. P. Shkarofsky, "Evaluation of multipole moments over the current density in a tokamak with magnetic probes," *Phys. Fluids*, vol. 25, p. 89, Jan. 1982.

[9] S. H. Seo, J. Kim, S. H. Huh, W. Choe, H. Y. Chang, and S.-H. Jeong, "Legendre polynomial expansion method for evaluating multipole moments of current density in toroidal devices," *Phys. Plasmas*, vol. 7, p. 1487, May 2000.

[10] R. C. Tautz and I. Lerche, "Bipolar solar magnetic fields—Behaviors resulting from a nonlinear force-free equation," *Astron. Astropphys.*, vol. 581, p. A6, 2015.

[11] R. D. Jackson, *Classical Electrodynamics*. Hoboken, NJ, USA: Wiley, 1962.

[12] N. N. Lebedev, *Special Functions*. New York, NY, USA: Dover, 1962.

[13] J. Blum, E. Lazzaro, J. O'Rourke, B. Keegan, and Y. Stephan, "Problems and methods of self-consistent reconstruction of tokamak equilibrium profiles from magnetic and polarimetric measurements," *Nucl. Fusion*, vol. 30, p. 1475, Aug. 1990.

[14] F. Alladio and F. Crisanti, "Analysis of MHD equilibria by toroidal multipolar expansions," *Nucl. Fusion*, vol. 26, no. 9, p. 1143, 1986.

[15] E. Lazzaro and P. Mantica, "Determination of equilibrium global parameters from external magnetic measurements in JET discharges with auxiliary heating," *Nucl. Fusion*, vol. 28, p. 913, May 1988.

[16] C. E. Shannon, "A mathematical theory of communication," *Bell Syst. Tech. J.*, vol. 27, no. 3, pp. 379–423, Jul./Oct. 1948.

[17] A. I. Khinchin, *Mathematical Foundations of Information Theory*. New York, NY, USA: Dover, 1963.

[18] J. R. Pierce, *An Introduction to Information Theory*. New York, NY, USA: Dover, 1980.

[19] S. Kullback and R. A. Leibler, "On information and sufficiency," *Ann. Math. Statist.*, vol. 22, no. 1, pp. 79–86, 1951.

[20] D. J. Galas, J. Dewey, J. Kunert-Graf, and N. A. Sakhanenko, "Expansion of the Kullback-Leibler divergence, and a new class of information metrics," *Axioms*, vol. 6, no. 2, p. 8, Apr. 2017, doi: 10.3390/axioms6020008.

[21] S. Zheng, "Course MTH 541/643: Statistical theory II," Dept. Math., Missouri State Univ., Springfield, MO, USA, Lecture Notes, 2020.

[22] N. Q. Nguyen, C. K. Abbey, and M. F. Insana, "Detectability index describes the information conveyed by sonographic images," in *Proc. IEEE Int. Ultrason. Symp.*, Oct. 2011, pp. 680–683.

[23] H. H. Barrett and K. J. Myers, *Foundations of Image Science*. Hoboken, NJ, USA: Wiley, 2004.

**Enzo Lazzaro** is a Plasma Physics Theorist, and presently an Associate Research Director of the Institute for Science and Technology of Plasma (ISTP), Consiglio Nazionale delle Ricerche (CNR), Milan, Italy. He is a former Director of the Institute of Plasma Physics, CNR. From 1981 to 1990, he was a Researcher in the Theory Division of JET-Joint Undertaking and since then actively involved in plasma theory (wave–plasma interactions, MHD, and dusty plasma) related to tasks of Eurofusion and other international collaborations, authoring and coauthoring about 300 articles.

**Luca Bonalumi** received the M.Sc. degree in plasma physics from the Università di Milano-Bicocca, Milan, Italy, in 2019.

**Silvana Nowak** is presently a First Researcher at ISTP-CNR, Milan, Italy. She has worked at CEA, France, and JET, U.K., where she is currently involved in several tasks of Eurofusion and other international collaborations.

**Daniele Brunetti** received the M.Sc. degree from the Università degli Studi di Milano, Milan, Italy, in 2010, and the Ph.D. degree from EPFL, Lausanne, Switzerland, in 2015.

He has worked on the tasks of Eurofusio at JET, U.K., and is currently a Researcher at CCFE, Culham, U.K.